ISSN 1674-1056
http://cpb.iphy.ac.cn
http://iopscience.iop.org/cpb
中国物理 B
Chinese Physics
中国物理 Chinese Physics B

Simulation of GaN micro-structured neutron detectors for improving electrical properties

Xin-Lei Geng(耿昕蕾)[1], Xiao-Chuan Xia(夏晓川)[1], Huo-Lin Huang(黄火林)[2], Zhong-Hao Sun(孙仲豪)[1], He-Qiu Zhang(张贺秋)[1], Xing-Zhu Cui(崔兴柱)[3], Xiao-Hua Liang(梁晓华)[3], Hong-Wei Liang(梁红伟)[1]
Citation: Chin. Phys. B, 2020, 29 (**2**): 027201 **doi:** 10.1088/1674-1056/ab671e
Journal homepage: http://cpb.iphy.ac.cn; http://iopscience.iop.org/cpb

What follows is a list of articles you may be interested in

Breakdown voltage enhancement in GaN channel and AlGaN channel HEMTs using large gate metal height

Zhong-Xu Wang(王中旭), Lin Du(杜林), Jun-Wei Liu(刘俊伟), Ying Wang(王颖), Yun Jiang(江芸), Si-Wei Ji(季思蔚), Shi-Wei Dong(董士伟), Wei-Wei Chen(陈伟伟), Xiao-Hong Tan(谭骁洪), Jin-Long Li(李金龙), Xiao-Jun Li(李小军), Sheng-Lei Zhao(赵胜雷), Jin-Cheng Zhang(张进成), Yue Hao(郝跃)
Chin. Phys. B . 2020, 29(2): 027301 . **doi:** 10.1088/1674-1056/ab5fb9

Tunneling magnetoresistance in ferromagnet/organic-ferromagnet/metal junctions

Yan-Qi Li(李彦琪), Hong-Jun Kan(阚洪君), Yuan-Yuan Miao(苗圆圆), Lei Yang(杨磊), Shuai Qiu(邱帅), Guang-Ping Zhang(张广平), Jun-Feng Ren(任俊峰), Chuan-Kui Wang(王传奎), Gui-Chao Hu(胡贵超)
Chin. Phys. B . 2020, 29(1): 017303 . **doi:** 10.1088/1674-1056/ab5d02

Tetraalkyl-substituted zinc phthalocyanines used as anode buffer layers for organic light-emitting diodes

Qian Chen(陈潜), Songhe Yang(杨松鹤), Lei Dong(董磊), Siyuan Cai(蔡思源), Jiaju Xu(许家驹), Zongxiang Xu(许宗祥)
Chin. Phys. B . 2020, 29(1): 017302 . **doi:** 10.1088/1674-1056/ab5933

Negative transconductance effect in p-GaN gate AlGaN/GaN HEMTs by traps in unintentionally doped GaN buffer layer

Mei Ge(葛梅), Qing Cai(蔡青), Bao-Hua Zhang(张保花), Dun-Jun Chen(陈敦军), Li-Qun Hu(胡立群), Jun-Jun Xue(薛俊俊), Hai Lu(陆海), Rong Zhang(张荣), You-Dou Zheng(郑有炓)
Chin. Phys. B . 2019, 28(10): 107301 . **doi:** 10.1088/1674-1056/ab3e00

Method of evaluating interface traps in Al_2O_3/AlGaN/GaN high electron mobility transistors

Si-Qin-Gao-Wa Bao(包斯琴高娃), Xiao-Hua Ma(马晓华), Wei-Wei Chen(陈伟伟), Ling Yang(杨凌), Bin Hou(侯斌), Qing Zhu(朱青), Jie-Jie Zhu(祝杰杰), Yue Hao(郝跃)
Chin. Phys. B . 2019, 28(6): 067304 . **doi:** 10.1088/1674-1056/28/6/067304

Simulation of GaN micro-structured neutron detectors for improving electrical properties*

Xin-Lei Geng(耿昕蕾)[1], Xiao-Chuan Xia(夏晓川)[1,†], Huo-Lin Huang(黄火林)[2], Zhong-Hao Sun(孙仲豪)[1], He-Qiu Zhang(张贺秋)[1], Xing-Zhu Cui(崔兴柱)[3], Xiao-Hua Liang(梁晓华)[3], and Hong-Wei Liang(梁红伟)[1,‡]

[1] *School of Microelectronics, Dalian University of Technology, Dalian* 116024, *China*
[2] *School of Optoelectronic Engineering and Instrumentation Science, Dalian University of Technology, Dalian* 116024, *China*
[3] *Institute of High Energy Physics, Chinese Academy of Sciences (CAS), Beijing* 100049, *China*

(Received 1 November 2019; revised manuscript received 29 November 2019; accepted manuscript online 3 January 2020)

Nowadays, the superior detection performance of semiconductor neutron detectors is a challenging task. In this paper, we deal with a novel GaN micro-structured neutron detector (GaN-MSND) and compare three different methods such as the method of modulating the trench depth, the method of introducing dielectric layer and p-type inversion region to improve the width of depletion region (W). It is observed that the intensity of electric field can be modulated by scaling the trench depth. On the other hand, the electron blocking region is formed in the detector enveloped with a dielectric layer. Furthermore, the introducing of p-type inversion region produces new p/n junction, which not only promotes the further expansion of the depletion region but also reduces the intensity of electric field produced by main junction. It can be realized that all these methods can considerably enhance the working voltage as well as W. Of them, the improvement on W of GaN-MSND with the p-type inversion region is the most significant and the value of W could reach 12.8 μm when the carrier concentration of p-type inversion region is 10^{17} cm^{-3}. Consequently, the value of W is observed to improve 200% for the designed GaN-MSND as compared with that without additional design. This work ensures to the researchers and scientific community the fabrication of GaN-MSND having superior detection limit in the field of intense radiation.

Keywords: GaN, micro-structured neutron detector, depletion region, electric field

PACS: 73.40.Kp, 73.61.Ey, 29.40.–n, 29.85.–c **DOI:** 10.1088/1674-1056/ab671e

1. Introduction

Due to the shortage and rising cost of ^{3}He gas, the application of ^{3}He proportional counters for detecting neutrons is restricted.[1] Si-based semiconductor neutron detectors have been utilized extensively as an alternative method for detecting neutrons during the past decade.[2–5] Nevertheless, they suffer radiation damage due to the small bandgap and displacement energy of Si.[6] With the development of wide bandgap semiconductors, GaN is considered to be the potential candidate for neutron detection under strong irradiation and high temperature conditions[7,8] due to its wide band gap (3.39 eV), high critical breakdown electric field (3×10^6 V/cm), large displacement energy (22 eV), high density (6.2 g/cm^{-3}) and good thermal stability (melting point: 2500 °C).[9–11] However, the detection performance such as detection efficiency and energy resolution of the neutron detector based on GaN is still not comparable to those based on Si,[12–14] which is due mainly to two reasons. (i) The planar structure is commonly employed in GaN neutron detectors, which cannot avoid the low detection efficiency restricted by the conflict between the long neutron mean free path and the short-charged particle range in neutron conversion layer.[15] (ii) The unintentionally doped GaN is usually of n-type with the background carrier concentration of $\sim 10^{16}$ cm^{-3}. Additionally residual shallow donors generated during material growth in the metal–organic chemical vapor deposition (MOCVD) or the hydride vapor phase epitaxy (HVPE),[15,16] bring difficulties for the enlargement in the width of depletion region (always only few micrometers).[17,18] Thus, it is urgently needed to find a solution for GaN-based neutron detectors that could overcome the shortcomings of the planar architecture and achieve a larger depletion region at the same background carrier concentration.

A novel GaN micro-structured neutron detector (GaN-MSND) is proposed in this paper. The advantages of GaN-MSND over the planar structure are analyzed and the significance of the wide depletion region for the detection performance is discussed in detail. Moreover, Sentaurus-TCAD software is utilized to investigate three methods such as the method of modulating trench depth, the method of introducing dielectric layer and p-type inversion region to improve the

*Project supported by the National Natural Science Foundation of China (Grant Nos. 11675198, 11875097, 11975257, 61774072, 61574026, and 61971090), the National Key Research and Development Program of China (Grant Nos. 2016YFB0400600 and2016YFB0400601), the Fundamental Research Funds for the Central Universities, China (Grant No. DUT19LK45), the China Postdoctoral Science Foundation (Grant No. 2016M591434), and the Science and Technology Plan of Dalian City, China (Grant No. 2018J12GX060).

†Corresponding author. E-mail: xiaochuan@dlut.edu.cn
‡Corresponding author. E-mail: hwliang@dlut.edu.cn

© 2020 Chinese Physical Society and IOP Publishing Ltd

width of depletion region of GaN-MSND. The mechanism and comparison of these methods are analyzed. It is expected that the GaN-MSND could enhance the detection efficiency of the planar neutron detector and achieve the superb detection performance with the improvement of the depletion region width. Consequently, such a novel strategy will be used in future to make the neutron detectors capable to cope with the extreme conditions.

2. Structures of GaN-MSND and simulation model

Figure 1 shows the schematic cross-section of the proposed GaN-MSND. The neutron converter of GaN-MSND is filled in the etched trenches and most of the reaction products generated at various depths of the neutron converter can enter into the adjacent detector. The neutron converter of planar neutron detector is commonly coated on the surface of GaN. The thick neutron converter can raise the chance of capturing neutron, but the entrance probability of the reaction products produced by the interaction between the neutron and the conversion material into the detector is reduced. This contradiction greatly limits the detection efficiency of planar neutron detector.[15] In contrast, the GaN-MSND has a larger amount of neutron converter filling and a wider contact area of neutron converter with the detector. Thus, the detection efficiency of GaN-MSND can be improved significantly.[19]

When the detector is operated at a reverse bias, the depletion region (near the p-GaN/i-GaN junction) is expanded obviously due to the large difference in concentration between p-GaN and i-GaN as marked in Fig. 1. The width of depletion region (W) has a significant importance for the detector because its value determines the detection performance of GaN-MSND such as charge collection efficiency and energy resolution.[20–23] A large width of depletion region can deposit more particle energy and improve the charge collection efficiency. Besides, the incomplete charge collection noise is reduced, which will result in the improvement of the energy resolution as can be seen from Eqs. (1) and (3).[21] Therefore, the method of creating a relatively large W is essential for obtaining GaN-MSND with superb detection performance. Operating the detector at a higher reverse bias is considered to be an easy way of increasing the W value.[24] However, an excessive high voltage will also lead to a high leakage current which can affect the system electronic noise and further degrade the detection performance such as energy resolution according to Eqs. (1) and (2).[21] The methods discussed in the next section focus on enhancing the operation voltage tolerance, by which a large depletion region can be achieved.

$$\mathrm{FWHM} = 2.35\sqrt{(\Delta E_1)^2 + (\Delta E_2)^2 + (\Delta E_3)^2}, \tag{1}$$

$$(\Delta E_1)^2 = (\Delta E_0)^2 + \left(\frac{2.35\mathrm{e}}{2q}\right)^2 \varepsilon^2 \tau I_\mathrm{d} + \frac{(2.35\mathrm{e})^2}{2q^2}\varepsilon^2 r_\mathrm{s}\left(\frac{T}{\tau}\right)\left(C_\mathrm{d}^2 + 2C_\mathrm{d}C_0\right), \tag{2}$$

$$\Delta E_2 = a(1-\gamma)E_\mathrm{r}^{1/2}, \tag{3}$$

where FWHM is the energy resolution; ΔE_1, ΔE_2, and ΔE_3 are the system electronic noise, incomplete charge collection noise, and carrier fluctuation noise, respectively; ΔE_0 is the electronic noise of preamplifier; e is 2.71828…; q is the electron charge; ε is the average ionizing energy; τ is the shaping time; I_d is the leakage current of the detector; r_s is the input impedance; C_d is the capacitance of the detector; C_0 is the capacitance of the gate–source field-effect transistor in the preamplifier; a is 0.5 for GaN; γ is the charge collection efficiency; E_r is the energy of the particle.

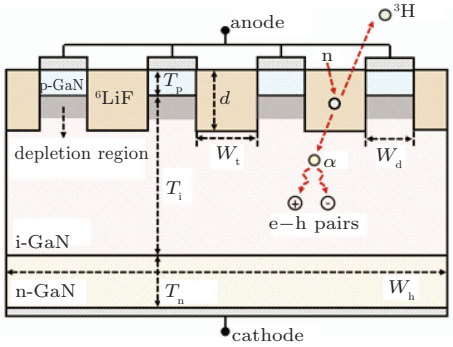


Fig. 1. Schematic drawing of GaN-MSND.

The simulations are performed by using the Sentaurus-TCAD. The doping-dependence and high-field-saturation models are employed for mobility. The Shockley–Read–Hall model is utilized to calculate the effect of charging and discharging of trap. To investigate the avalanche breakdown effect in the detector, the Selberherr's impact ionization model is used to simulate the reverse characteristics.

Figure 2(a) shows the simulation results of the electric field distribution in a specific GaN-MSND. The structural parameters used in simulation are listed in Table 1. The anode and cathode of the device are formed as Ohmic contacts on p-GaN and n-GaN. The maximum working voltage (V_r) is defined at the current density $I = 1 \times 10^{-6}$ mA/mm, where the leakage level is considered to be an acceptable level as shown in many researches.[18,25] Figure 2(b) shows the electric field profile extracted along the x-cut marked in Fig. 2(a). The electric field reaches a maximum value at the p-GaN/i-GaN junction and decreases linearly to 0 V/cm in the i-GaN. Parameter W is defined as the distance between the p-GaN/i-GaN interface and the 0 V/cm position. Thus, the specific GaN-MSND without additional design has a W value of 3.9 μm at V_r of 150 V.

Table 1. Structural parameters of GaN-MSND adopted in the work.

Parameters	Descriptions	Values
W_t	Width of trench	15 μm
W_d	Distance between the adjacent trench	5 μm
W_h	Length of GaN-MSND	85 μm
d	Depth of trench	1.5 μm
T_n	Thickness of n-GaN	2 μm
T_i	Thickness of i-GaN	20 μm
T_p	Thickness of p-GaN	500 nm
N_n	Density of electron in the n-GaN	5×10^{18} cm^{-3}
N_i	Density of electron in the i-GaN	1×10^{16} cm^{-3}
N_p	Density of hole in the p-GaN	1×10^{17} cm^{-3}

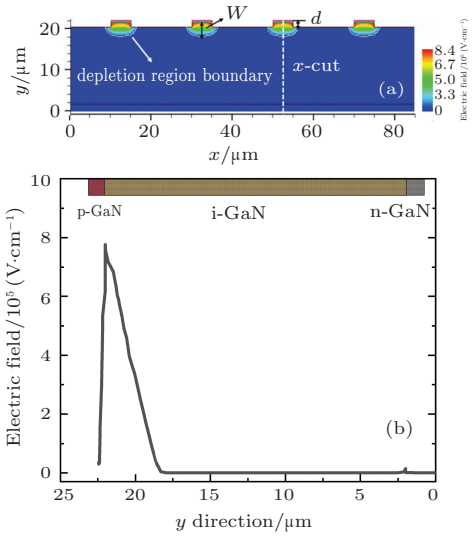


Fig. 2. (a) Electric field distribution in GaN-MSND at $V_r = 150$ V, and (b) electric field profile of GaN-MSND extracted along vertical direction (x-cut).

3. Results and discussion

3.1. Influence of modulating trench depth on W of GaN-MSND

The trenches filled with neutron convert material ^{6}LiF which plays a role of transferring the neutrons into the charged particles are crucial for the GaN-MSND. It should be noted that the modulation of the trench depth d (as shown in Fig. 1) is an effective way to improve V_r and W of the device. The plots of simulated reverse I–V characteristics and the corresponding results of the V_r and W *versus* d in a range from 0.5 μm to 7.5 μm in GaN-MSND are illustrated in Fig. 3. The increase of d can lead both W and V_r (defined at the current reaches 10^6 mA/mm) to be improved, but the additional etching depth to have no obvious effect when d reaches 5.5 μm. Considering the feasibility of the device fabrication, d is set to be 5.5 μm, by which V_r and W can reach 226 V and 4.7 μm, respectively.

To explain the changing trend of V_r, the distribution of electric field of the device is analyzed. Figure 4 demonstrates the electric field profile extracted by taking a y-cut along the bottom of their trenches with the applied reverse voltage of 60 V. The peaks of the electric field occur at the trench corners, which are caused by the large curvature of electric field line. In addition, these values become lower as the distance between trench corner and the p-GaN/i-GaN junction increases, which contributes to the improvement of V_r.[26] However, when d reaches 5.5 μm, the trench corners are located in the non-depletion region without high electric field, which has no effect on the electric field distribution near the junction. Therefore, neither V_r nor W will continue to change with d.

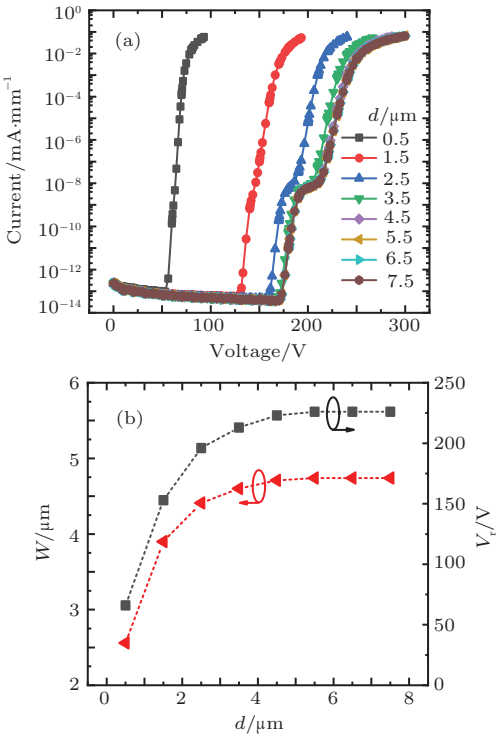


Fig. 3. (a) Reverse characteristics of GaN-MSND *versus* voltage for various d values, and (b) W and V_r extracted from the simulation results *versus* d.

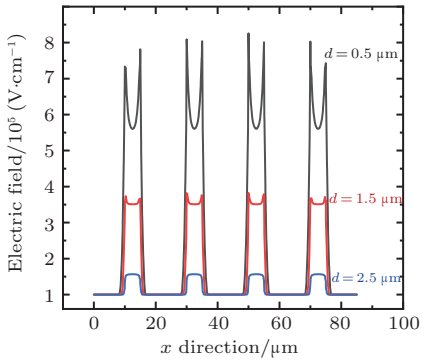


Fig. 4. Profiles of electric field *versus* x for GaN-MSND for d values of 0.5 μm, 1.5 μm, and 2.5 μm at the depth of respective trench bottom when the reverse voltage is 60 V.

3.2. Influence of dielectric layer on W of GaN-MSND

Based on the optimized results, a possible method to further improve V_r and W is to introduce a dielectric layer on the trench surface as shown in Fig. 5. Single-layered SiO_2 or Al_2O_3 with a thickness of 0.5 μm is adopted and their effects on V_r and W of GaN-MSND are compared in the simulation. The density of fixed charges Q_f at the dielectric/GaN

interface is calibrated by the reported value in the literature: for the interface of SiO_2/GaN, the positive Q_f is set to be 3×10^{11} cm^{-2};[27,28] for Al_2O_3/GaN, the unusual negative Q_f at the interface due to the O-rich region near the interface caused by Al vacancy and O interstitial has been reported.[29] And its value of 2×10^{12} cm^{-2} is employed in this work.[30,31]

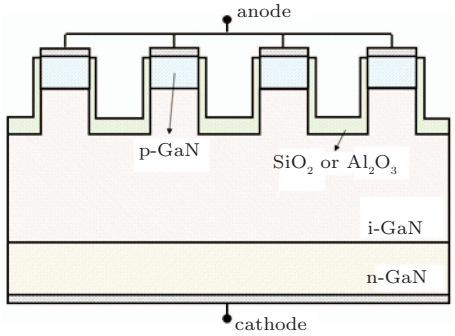


Fig. 5. Schematic diagram of GaN-MSND with trench surface covered by dielectric layer.

Figure 6 shows the reverse *I*–*V* characteristics of GaN-MSND with SiO_2 or Al_2O_3 layer, and the corresponding V_r is extracted to be 167 V and 270 V, respectively. Compared with the optimized results above, the V_r of GaN-MSND with SiO_2 decreases while that with Al_2O_3 increases. The negative Q_f at the Al_2O_3/GaN interface leads the conduction band to bend up, where the electrons are blocked. The electrons blocking region can drive the electrons far from the Al_2O_3/GaN interface as well as reduce the leakage current along the trench sidewalls of GaN-MSND as shown in Fig. 7(a).

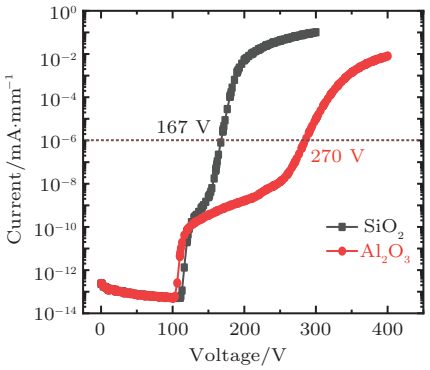


Fig. 6. Reverse characteristics of GaN-MSND with SiO_2 with a positive fixed charge density of 3×10^{11} cm^{-2} on GaN/SiO_2 interface and with Al_2O_3 with a negative fixed charge density of 2×10^{12} cm^{-2} on GaN/Al_2O_3 interface.

Conversely, the electron accumulation region is formed near the trench surface due to the positive Q_f at the SiO_2/GaN interface, which is the main factor of increasing the surface leakage along the sidewalls and reducing the V_r as shown in Fig. 7(b). Therefore, we can conclude that the introduction of 0.5 μm-Al_2O_3 as the dielectric layer of GaN-MSND can increase V_r to 270 V and the width of depletion region W to 6.2 μm as shown in Fig. 8.

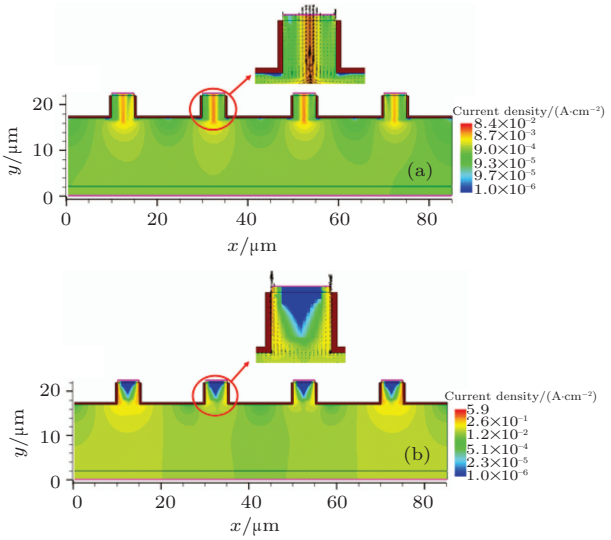


Fig. 7. Current density distribution for GaN-MSND with (a) Al_2O_3 and (b) SiO_2.

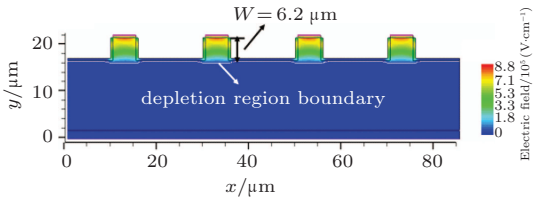


Fig. 8. Electric field distribution for GaN-MSND with Al_2O_3 at V_r of 270 V.

3.3. Influence of p-type inversion region on *W* of GaN-MSND

The introducing of p-type inversion layer is another way to increase V_r and W as shown in Fig. 9. The thickness of p-type inversion region is set to be 0.5 μm. The reverse characteristics of GaN-MSND with a p-GaN carrier concentration N_p of 1×10^{16} cm^{-3}, 3×10^{16} cm^{-3}, 5×10^{16} cm^{-3}, 7×10^{16} cm^{-3}, 9×10^{16} cm^{-3}, and 1×10^{17} cm^{-3} are illustrated in Fig. 10(a). The V_r values are obtained as follows: 306 V, 436 V, 595 V, 782 V, 1000 V, and 1112 V, which indicates a significant enhancement in V_r compared with the former results. Besides, with the increase of N_p, the improvement of W is significant as well, as demonstrated in Fig. 10(b). When N_p is increased to 1×10^{17} cm^{-3}, W is enhanced up to 12.8 μm, which is more than twice the W of GaN-MSND with Al_2O_3 layer.

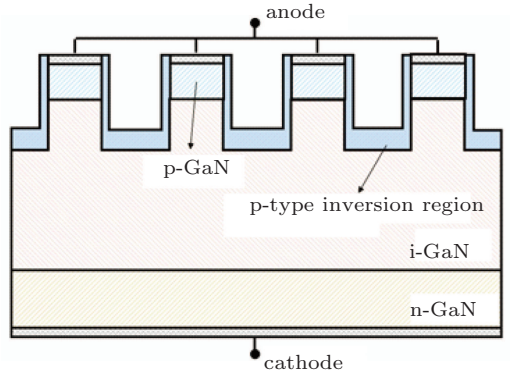


Fig. 9. Schematic drawing of GaN-MSND with p-type inversion region.

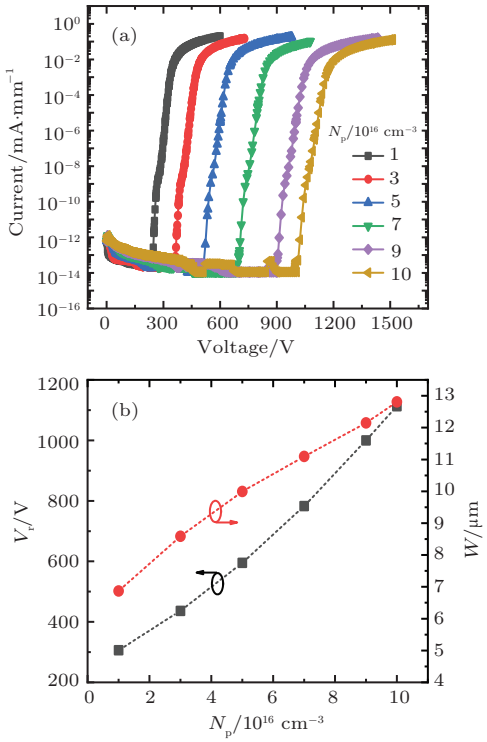


Fig. 10. (a) Reverse characteristics of GaN-MSND with N_p of 1×10^{16} cm^{-3}, 3×10^{16} cm^{-3}, 5×10^{16} cm^{-3}, 7×10^{16} cm^{-3}, 9×10^{16} cm^{-3}, and 1×10^{17} cm^{-3} and (b) relationship between V_r and N_p, and W and N_p for GaN-MSND with p-type inversion region.

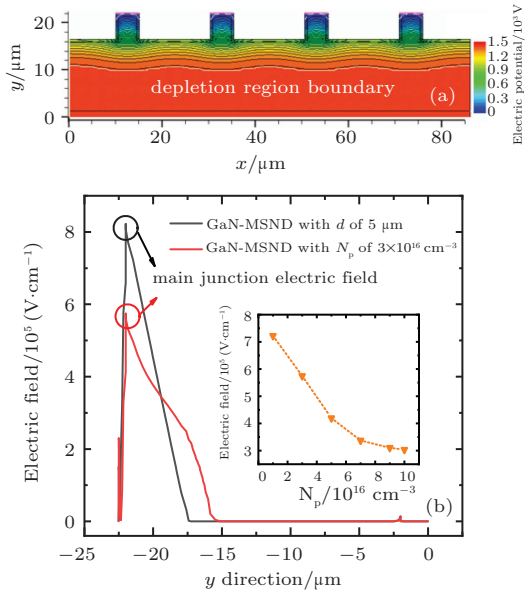


Fig. 11. (a) Potential distribution for GaN-MSND with N_p of 1×10^{17} cm^{-3} at reverse voltage of 1000 V, and (b) electric field profile for GaN-MSND with d of 0.5 μm and N_p of 3×10^{16} cm^{-3} at $x=32.5$ μm when reverse voltage is 200 V. The inset shows the main junction electric field varying with N_p at reverse voltage of 200 V for GaN-MSND.

Figure 11(a) shows the potential distribution of GaN-MSND with p-type inversion region. The p-type inversion region and the i-GaN form new p/n junctions and due to the continuity of potential, the potential is re-arranged and extended to the initially un-depleted region in i-GaN,[32] thus improving the width of depletion region. Besides, a lower electric field peak exists at the main junction with the assistance of the extension of depletion region as demonstrated in Fig. 11(b), which suggests an enhancement in V_r as well as W. The inset of Fig. 11(b) shows the relationship between N_p and electric field at the main junction. It should be noted that the electric field peak decreases as N_p increases, and hence, V_r increases accordingly.

The GaN-MSND with p-type inversion region can significantly improve V_r and W, but the vertical p-type inversion region on the sidewall of GaN-MSND is not easy to realize in the device process. Considering the achievability of the process, the sidewalls are further etched into trapezoids so that the p-type region could easily be formed by ion implantation. The GaN-MSND, of which N_p is 1×10^{17} cm^{-3}, with the trapezoidal sidewalls is simulated and its V_r and W are improved to 1342 V and 13.6 μm as shown in Fig. 12, which may be attributed to the larger contact area between p-type inversion region and i-GaN.

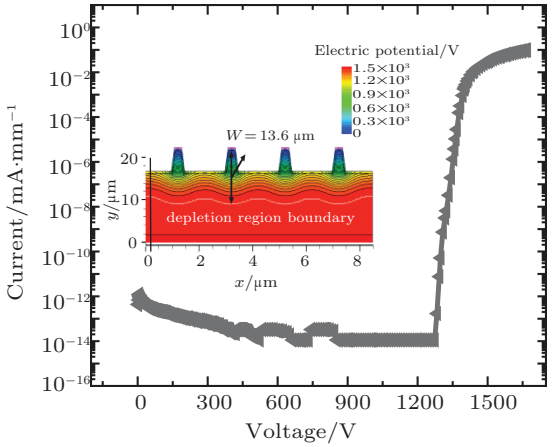


Fig. 12. Reverse characteristic of GaN-MSND with trapezoidal p-type inversion region of which N_p is 1×10^{17} cm^{-3}, with the inset showing its potential distribution at reverse voltage of 1342 V.

3.4. Comparison among three methods to improve W

The transport distance of the charged particles in GaN depends on their energy. Upon absorbing a neutron, the ^{6}LiF fissions into two reaction products, *i.e.* an alpha particle (2.06 MeV) and a ^{3}H particle (2.73 MeV).[12] Since the energy loss per unit distance of alpha particle in GaN is larger than that of ^{3}H, only the alpha particles incident into the detector is considered, while ^{3}H is supposed to go throughout the device. The electron–hole pairs are generated as the alpha particles pass through the depletion region and drift towards respective electrodes by the electric field. The alpha particles with 2.06 MeV have a transport distance of approximately 5 μm in GaN. Therefore, for a given$d$ of 5.5 μm, W should be at least 10.5 μm so that the detector can collect the alpha particles generated at the bottom of the trenches. As mentioned above, the GaN-MSND without additional design has a maximum W value of 4.7 μm by modulating the trench depth, while adding Al_2O_3 layer could increase W value to 6.2 μm. In contrast, the GaN-MSND with p-type inversion region has a largest W value of 12.8 μm and thus, it could be the

most appropriate method to fabricate the detector with high detection performance.

4. Conclusions

In this work, three methods of improving W value of GaN-MSND is proposed and analyzed. For GaN-MSND with d value of 5.5 μm, W value increases to 4.7 μm at a V_r value of 226 V. The W value is further improved to 6.2 μm for GaN-MSND with the Al_2O_3 layer at V_r of 270 V. Moreover, GaN-MSND with the p-GaN inversion region can have a W value of 12.8 μm when N_p is 1×10^{17} cm^{-3} at V_r of 1112 V. This study not only provides a series of pathways to obtaining GaN-MSND with better detection performance through the enhancement of the depletion region but also points out the GaN-MSND applications in the field of neutron detection in intense radiation environment.

References

[1] Ochs T R, Bellinger S L, Fronk R G, Henson L C, Huddleston D E, Lyric Z I, Shultis J K, Smith C T, Sobering T J and McGregor D S 2017 *IEEE Trans. Nucl. Sci.* **64** 1846

[2] McGregor D S, Bellinger S L and Shultis J K 2013 *J. Cryst. Growth* **379** 99

[3] Shao Q, Voss L F, Conway A M, Nikolic R J, Dar M A and Cheung C L 2013 *Appl. Phys. Lett.* **102** 063503

[4] Huang K C, Dahal R, Lu J J Q, Danon Y and Bhat I B 2013 *Appl. Phys. Lett.* **102** 152107

[5] Voss L F, Reinhardt C E, Graff R T, Conway A M, Nikolić R J, Deo N and Cheung C L 2010 *J. Electron. Mater.* **39** 263

[6] Millan J, Godignon P, Perpina X, Perez-Tomas A and Rebollo J 2014 *IEEE Trans. Power Electron.* **29** 2155

[7] Lü L, Zhang J C, Xue J S, Ma X H, Zhang W, Bi Z W, Zhang Y and Hao Y 2012 *Chin. Phys. B* **21** 037104

[8] Mulligan P, Qiu J, Wang J H and Cao L R 2014 *IEEE Trans. Nucl. Sci.* **61** 2040

[9] Shur M 2019 *Solid-State Electron.* **155** 65

[10] Xu K, Wang J F and Ren G Q 2015 *Chin. Phys. B* **24** 066105

[11] Sellin P J and Vaitkus J 2006 *Nucl. Instrum. Methods Phys. Res., Sect. A* **557** 479

[12] Mulligan P, Wang J H and Cao L 2013 *Nucl. Instrum. Methods Phys. Res., Sect. A* **719** 13

[13] Melton A G, Burgett E, Xu T M, Hertel N and Ferguson I T 2012 *Physica Status Solidi* **9** 957

[14] Atsumi K, Inoue Y, Mimura H, Aoki T and Nakano T 2014 *APL Mater.* **2** 032106

[15] Wang J H, Mulligan P, Brillson L and Cao L R 2015 *Appl. Phys. Rev.* **2** 031102

[16] Morkoc H 2001 *Mater. Sci. Eng. R-Rep.* **33** 135

[17] Vaitkus J, Cunningham W, Gaubas E, Rahman M, Sakai S, Smith K M and Wang T 2003 *Nucl. Instrum. Methods Phys. Res., Sect. A* **509** 60

[18] Owens A, Barnes A, Farley R A, Germain M and Sellin P J 2012 *Nucl. Instrum. Methods Phys. Res., Sect. A* **695** 303

[19] Nikolic R J, Cheung C L, Reinhardt C E and Wang T F 2005 *Optoelectronic Devices: Physics, Fabrication, and Application II*, 24 October, 2005, Boston, USA, p. 36

[20] Xu Q, Mulligan P, Wang J H, Chuirazzi W and Cao L 2017 *Nucl. Instrum. Methods Phys. Res., Sect. A* **849** 11

[21] Wang G, Fu K, Yao C S, Su D, Zhang G G, Wang J Y and Lu M 2012 *Nucl. Instrum. Methods Phys. Res., Sect. A* **663** 10

[22] Ye X, Xia X C, Liang H W, Li Z, Zhang H Q, Du G T, Cui X Z and Liang X H 2018 *Chin. Phys. B* **27** 087304

[23] Lu M, Zhang G G, Fu K and Yu G H 2010 *Chin. Phys. Lett.* **27** 052901

[24] Sze S M and Ng K K 2006 *Physics of semiconductor devices*, 3rd edn. (Hoboken: John Wiley & Sons) p. 83

[25] Zhu Z F, Zhang H Q, Liang H W, Tang B, Peng X C, Liu J X, Yang C, Xia X C, Tao P C, Shen R S, Zou J J and Du G T 2018 *Nucl. Instrum. Methods Phys. Res., Sect. A* **893** 39

[26] Xie G, Xu E, Hashemi N, Zhang B, Fu F Y and Ng W T 2012 *Chin. Phys. B* **21** 086105

[27] Truyen N X, Taoka N, Ohta A, Makihara K, Yamada H, Takahashi T, Ikeda M, Shimizu M and Miyazaki S 2018 *Jpn. J. Appl. Phys.* **57** 04FG11

[28] Ohta A, Truyen N X, Fujimura N, Ikeda M, Makihara K and Miyazaki S 2018 *Jpn. J. Appl. Phys.* **57** 06KA08

[29] Cho Y J, Chung K B and Chang H S 2018 *Thin Solid Films* **649** 57

[30] Jackson C M, Arehart A R, Cinkilic E, McSkimming B, Speck J S and Ringel S A 2013 *J. Appl. Phys.* **113** 204505

[31] Biswas D, Torii N, Fujita H, Yoshida T, Kubo T and Egawa T 2019 *Semicond. Sci. Technol.* **34** 055014

[32] Udrea F, Deboy G and Fujihira T 2017 *IEEE Trans. Electron Dev.* **64** 713